Mesoionic pyridopyrimidinylium and pyridooxazinylium olates and non-mesoionic pyridopyrimidinones. Structures in the solid state, solution, and matrices†

Carsten Plüg,[a] Bianca Wallfisch,[a] Heidi Gade Andersen,[a] Paul V. Bernhardt,[a] Lisa-Jane Baker,[b] George R. Clark,[b] Ming Wah Wong[a,c] and Curt Wentrup*[a]

[a] *Chemistry Department, The University of Queensland, Brisbane, Qld 4072, Australia. E-mail: wentrup@chemistry.uq.edu.au*
[b] *Chemistry Department, University of Auckland, Private Bag 92019, Auckland, New Zealand*
[c] *Chemistry Department, National University of Singapore, Kent Ridge, Singapore 119260*

Received (in Cambridge, UK) 16th May 2000, Accepted 28th July 2000
Published on the Web 21st September 2000

X-Ray crystal structures, ^{13}C NMR spectra and theoretical calculations (B3LYP/6-31G*) are reported for the mesoionic (zwitterionic) pyridopyrimidinylium- and pyridooxazinyliumolates **2a**, **3a** and **5a**,**b** as well as the enol ether **11b** and the enamine **11c**. The 1-NH compounds like **1a**, **2a** and **3a** exist in the mesoionic form in the crystal and in solution, but the OH tautomers such as **1b** and **2b** dominate in the gas phase as revealed by the Ar matrix IR spectra in conjunction with DFT calculations. All data indicate that the mesoionic compounds can be regarded as intramolecular pyridine–ketene zwitterions (*cf.* **16** → **17**) with a high degree of positive charge on the pyridinium nitrogen, a long pyridinium N–CO bond (*ca.* 1.44–1.49 Å), and normal C=O double bonds (*ca.* 1.22 Å). All mesoionic compounds exhibit a pronounced tilting of the "olate" C=O groups (the C=O groups formally derived from a ketene) towards the pyridinium nitrogen, giving NCO angles of 110–118°. Calculations reveal a hydrogen bond with 6-CH, analogous to what is found in ketene–pyridine zwitterions and the C_3O_2–pyridine complex. The 2-OH tautomers of type **1b**, **2b**, and **11** also show a high degree of zwitterionic character as indicated by the canonical structures **11** ↔ **12**.

Introduction

The structure of Chichibabin's (Tschitschibabin's) "malonyl α-aminopyridine"[1] **1** has long been of interest to chemists.[2] In the 1960s, Katritzky and Waring proposed, on the basis of UV and IR spectroscopic data, that **1** exists in the mesoionic (zwitterionic) form **1a** (Chart 1) in solution.[3] Other possibilities, **1b**–**d** were ruled out. The mesoionic form **1a** was subsequently confirmed by ^1H NMR measurements, although the resonance of the interesting "mesoionic" proton on 1-N was not observed.[4] We have located this signal at 12.04 ppm in DMSO-d_6 solution. Simonsen confirmed the mesoionic structure **1a** in the solid state by X-ray crystallography.[5] This was a considerable achievement because, as we have experienced, it can be rather difficult to obtain useful crystals of mesoions of type **1**. It is presumably for this reason that no other X-ray data for NH mesoions of this type can be found in the literature. Although previously ruled out, we will show in this paper that the non-mesoionic form **1b** can nevertheless be stabilised in matrices.

It is desirable to obtain X-ray data for mesoionic heterocycles of type **1** because the structures are in fact rather unusual, with the C=O group tilted towards the nitrogen atom at the ring junction; furthermore, the "amide type" N–CO bonds are unusually long, of the order 1.44–1.50 Å, *i.e.* they are long N–C single bonds showing no sign of an amide type conjugation. This phenomenon appears to be general in mesoionic compounds possessing comparable structural elements.‡

Here we report the synthesis of the mesoionic pyridopyrimidinyliumolates **2a** and **4b**, and the pyridooxazinyliumolate **5a**, a detailed analysis of the ^1H and ^{13}C NMR spectra of **2a**, **3a**, **4a**–**c** and **5a**,**b**, X-ray crystal structures for **2a**, **3a** and **5a**,**b**, and matrix IR studies demonstrating the existence of the elusive OH-tautomers **1b** and **2b**. NMR spectra and X-ray structures of the "fixed enols" and enamine **11a**–**c** are also reported and reveal that these compounds too are highly zwitterionic. DFT calculations are in excellent agreement with the ^{13}C NMR interpretations, the structures, and the IR assignments. The question of valence tautomerisation between mesoionic compounds of these types and open-chain ketene isomers is addressed in a separate paper.[6]

Results and discussion

Compounds **2a** and **3**–**5** were synthesised by treatment of 2-aminopyridine or 2-pyridone with the requisite 2-substituted malonic acid. While better yields may be obtainable using Kappe's "magic malonate" (2,4,6-trichlorophenyl malonate) method,[7] the malonoyl chloride–chlorocarbonylketene method[8] is more convenient and was adopted here. Other pyridopyrimidinylium-[9] and pyridooxazinyliumolates[10] have been prepared from C_3O_2 or chlorocarbonylketenes and the appropriate 2-aminopyridine or 2-pyridone.

† Calculated IR spectral data and Cartesian coordinates for **1a**–**d**, **2a**–**c**, **4a**,**b**, **5a**, **11a**,**b**, and NBO charges for **1a**–**d**, **4b**, and 2-aminopyridine, X-ray crystallographic bond lengths and angles, a table and figures showing intermolecular H-bonding and crystal packing are available as supplementary data. For direct electronic access see http://www.rsc.org/suppdata/p2/b0/b003933k/

‡ Key N–CO bond lengths and NCO angles are indicated in the formulas in Chart 1 for ease of reference.

 DOI: 10.1039/b003933k

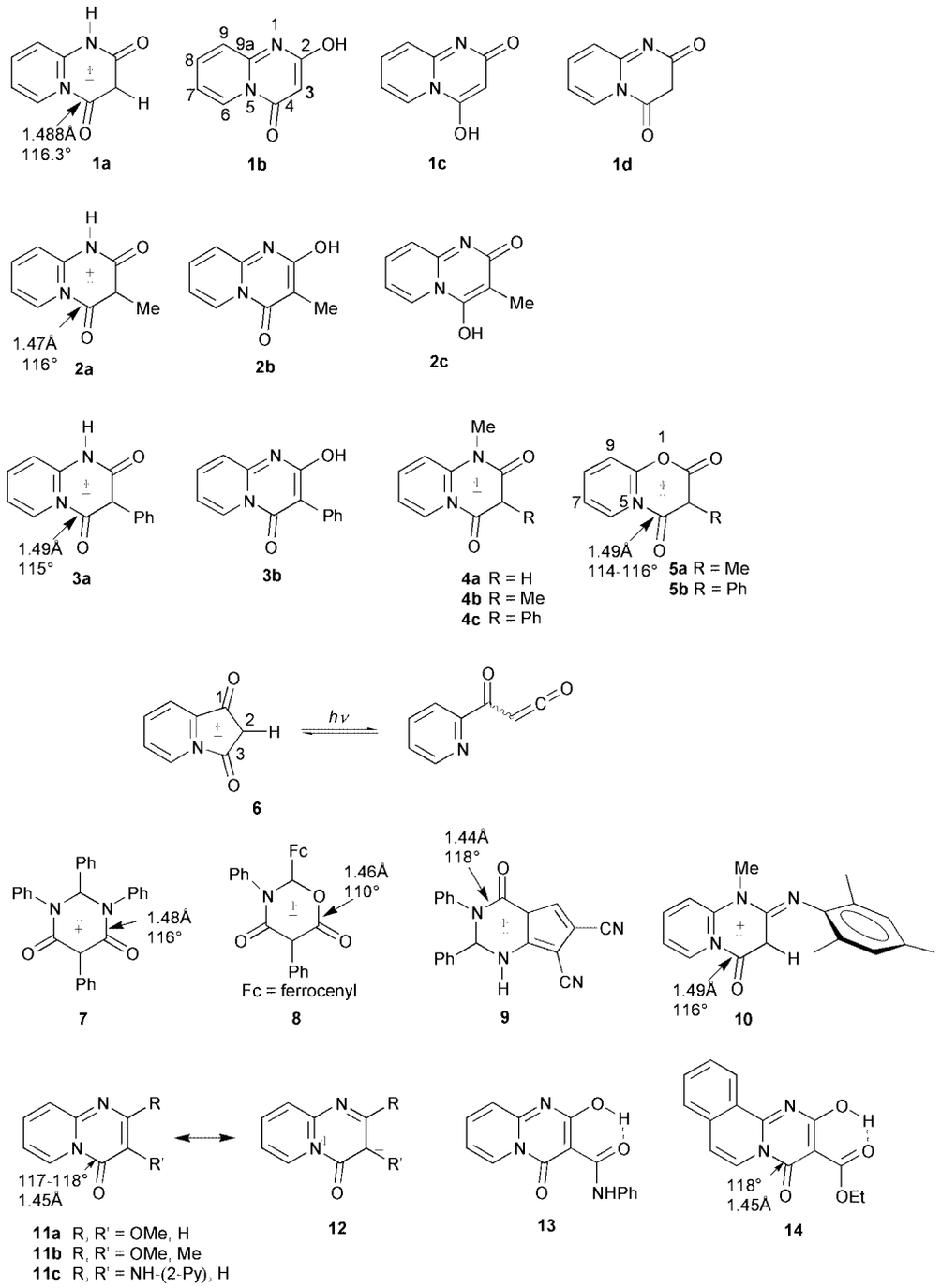

Chart 1

NMR data

The ^{1}H and ^{13}C NMR data for several compounds are given in Charts 2 and 3 together with calculated data (GIAO-B3LYP). It is seen that already the B3LYP/6-31G* level gives good agreement with experiment, and that this improved further at the GIAO-B3LYP/6-311G**//SCRF-B3LYP/6-31G* level. In order to test the validity of B3LYP calculations for charged compounds, we have also calculated the ^{13}C NMR chemical shifts for several carbanions,[11] pyridinium ylides[12] known in the literature, and the mesoionic compound **6** prepared in our laboratory.[13] Some of these data are collected in Chart 4. It can be concluded that B3LYP is extraordinarily reliable and therefore a valuable tool for the assignment of ^{13}C NMR data of carbanionic and zwitterionic compounds. However, it is seen from Charts 2 and 3 that both the ^{1}H and the ^{13}C NMR data of mesoions like **1a** and **2a** are very similar to those of the OH-tautomers like **2b**, and it would be very difficult to make a distinction on this basis without the help of the calculated data. The good agreement obtained for the "fixed" mesoions (**4a**–**c**, **5a**,**b**) and the enol ethers **11a**,**b** permit the conclusion that compounds **1** and **2** are more likely to exist in the mesoionic forms **1a** and **2a** than the enol forms **1b** and **2b** in solution. The main differences between mesoions of type **1a**,**2a**,**3a** or **4** on the one hand and enols of type **1b**,**2b**,**3b** or enol ethers and enamines **11** on the other lie in the chemical shifts of 2-C and 9-C. The carbonyl carbon 2-C in the mesoions comes at higher field than the "enol" carbons in **2b** or **11a**,**b**. The aromatic 9-C appears at significantly higher field in the mesoions than in the "enols". These differences support the conclusion that **1**, **2**, and **3** exist in the mesoionic forms in solution (**1a**, **2a**, **3a**). An important characteristic in the ^{13}C NMR spectra of all the mesoionic compounds is the fact that 8-C (a pyridine-γ type carbon) appears at lower field than 6-C (a pyridine-α type carbon) as is typical of pyridinium compounds. The same observation applies to the recently described pyrrolo[1,2-*a*]pyridinyl-

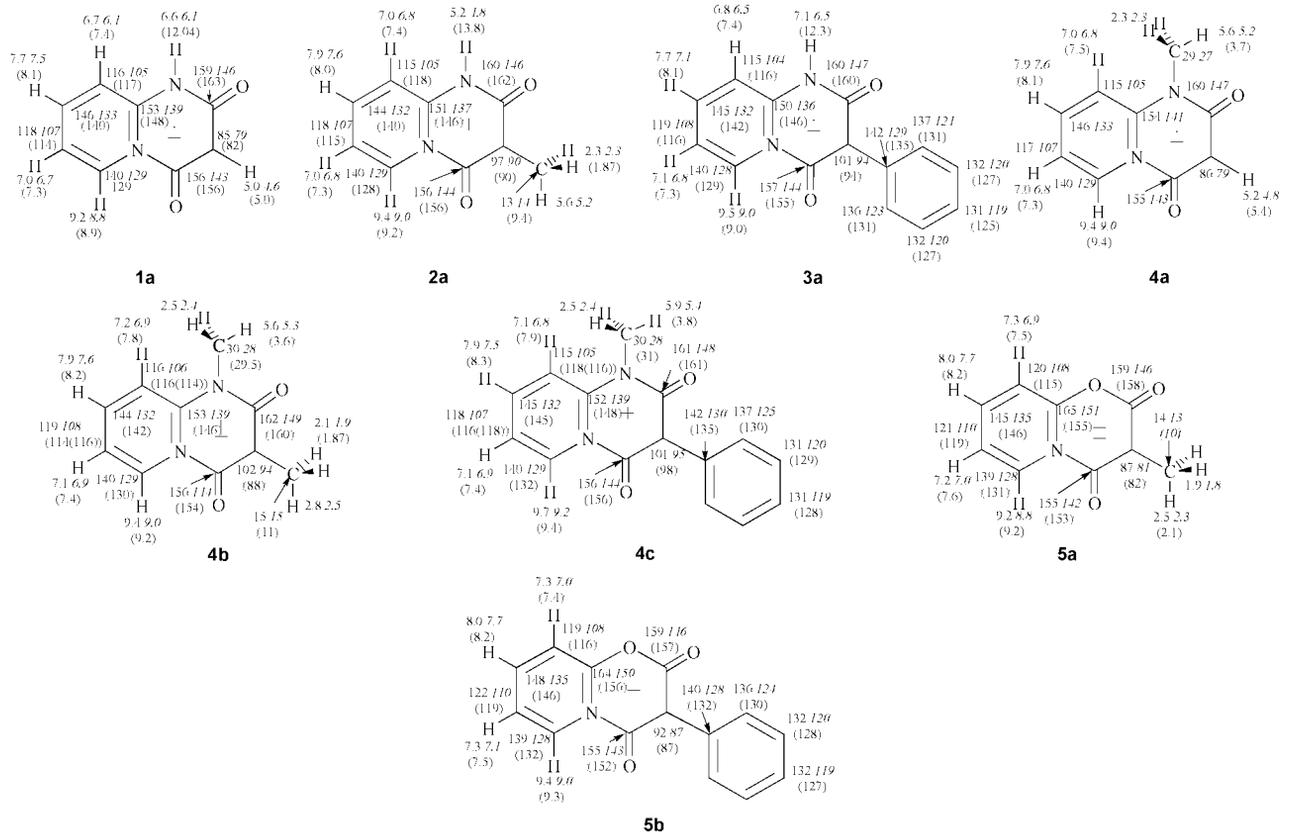

Chart 2 Calculated (B3LYP/6-31G* and B3LYP/6-311G**) and experimental ^{13}C chemical shifts of mesoions (in ppm relative to TMS). B3LYP/6-31G* values are in italics and experimental values in parentheses.

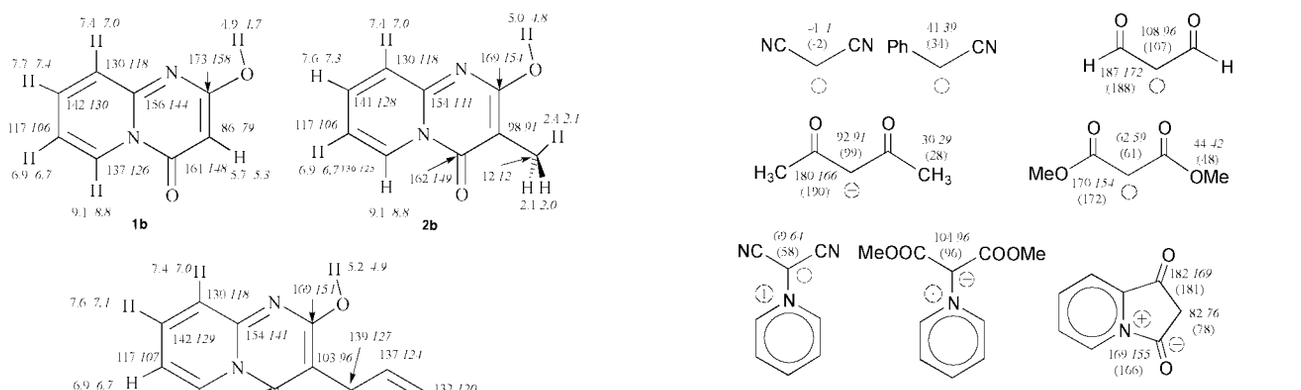

Chart 3 Calculated (B3LYP/6-31G* and B3LYP/6-311G**) and experimental ^{13}C chemical shifts of non-mesoionic compounds in ppm relative to TMS. B3LYP/6-31G* values are in italics and experimental values in parentheses.

Chart 4 Calculated and experimental ^{13}C chemical shifts of carbanions, pyridine ylides and mesoion **6**. Calculated data by B3LYP/6-311G** (upright) and B3LYP/6-31G* (italics); experimental values in ppm relative to TMS (in parentheses).

iumolates **6**.[13] Note however that this is also true of the calculated data for **2b** as well as the experimental data for **11** and is in agreement with the zwitterionic character of these compounds as described below. Carbon 3 in all these compounds is strongly carbanionic and gives rise to a signal at high field; this also causes the resonances of the flanking carbonyl carbons to appear at relatively high fields. Thus, the ^{13}C NMR spectra are in agreement with structures that can be described as pyridinium compounds, with a high degree of localisation of positive charge on the pyridine nitrogen, and the negative charge in the malonyl fragment (*cf.* structures **17** and **19** described below).

In the ^{1}H NMR spectra, the resonances of the NH protons appear at very low field, 12–14 ppm (*ca.* 1 ppm lower field in $CDCl_3$ than in DMSO).

X-Ray structures

The X-ray structures of **2a**, **3a** and **5a**,**b** are shown in Figs. 1–4. Initial attempts to grow suitable crystals of **2a** and **3a** failed because, although suitable crystals can be grown from DMSO solution, for example, they deteriorate as soon as the solvent is filtered off. The successful diffractions of **2a** and **3a** were obtained on wet crystals, protected by and mounted in oil or

silicone grease. One of the most interesting aspects of the structures is the tilting of the C=O groups at 4-C towards the ring junctions (5-N) and the lengthening of the "amide" N(5)–CO bonds. Thus, the NCO angles are always 114–116° in these compounds, and the N–CO bond lengths are 1.47–1.49 Å. A normal amide C–N bond length is 1.35 Å; the longest known is 1.475 Å in 1-azaadamantan-2-one where conjugation is drastically reduced due to twisting.[14] The other amide bonds in **2a** and **3a**, N(1)–C(2), and the corresponding lactone bonds in **5** are more normal at 1.39–1.44 Å, but the C=O groups at 2-C show just as much tilting towards 1-N or 1-O (113–118° in all the compounds examined here).

The structures indicate the presence of a rather unusual hydrogen bond C(6)–H(6)···O(4) with a bond length of 2.2–2.3 Å in the six structures investigated here (see the supplementary data). The calculations faithfully reproduce all the distortions, with H-bond lengths of *ca.* 2.2 Å (Chart 5). This

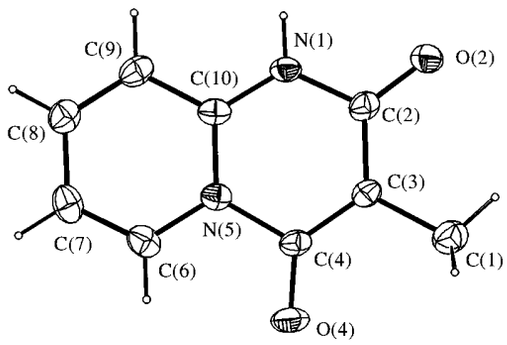

Fig. 1 ORTEP diagram of **2a**.

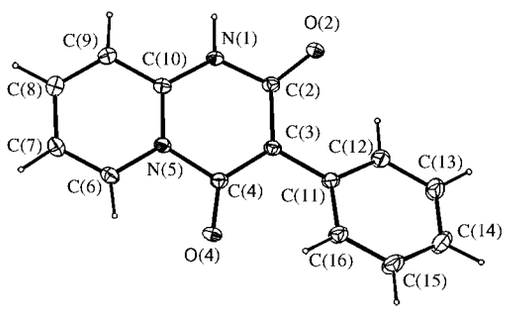

Fig. 2 ORTEP diagram of **3a**.

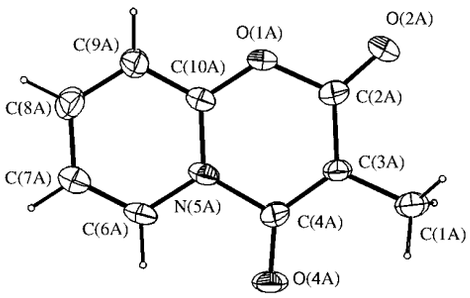

Fig. 3 ORTEP diagram of **5a**.

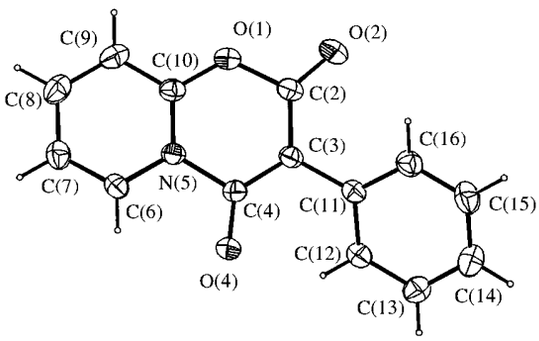

Fig. 4 ORTEP diagram of **5b**.

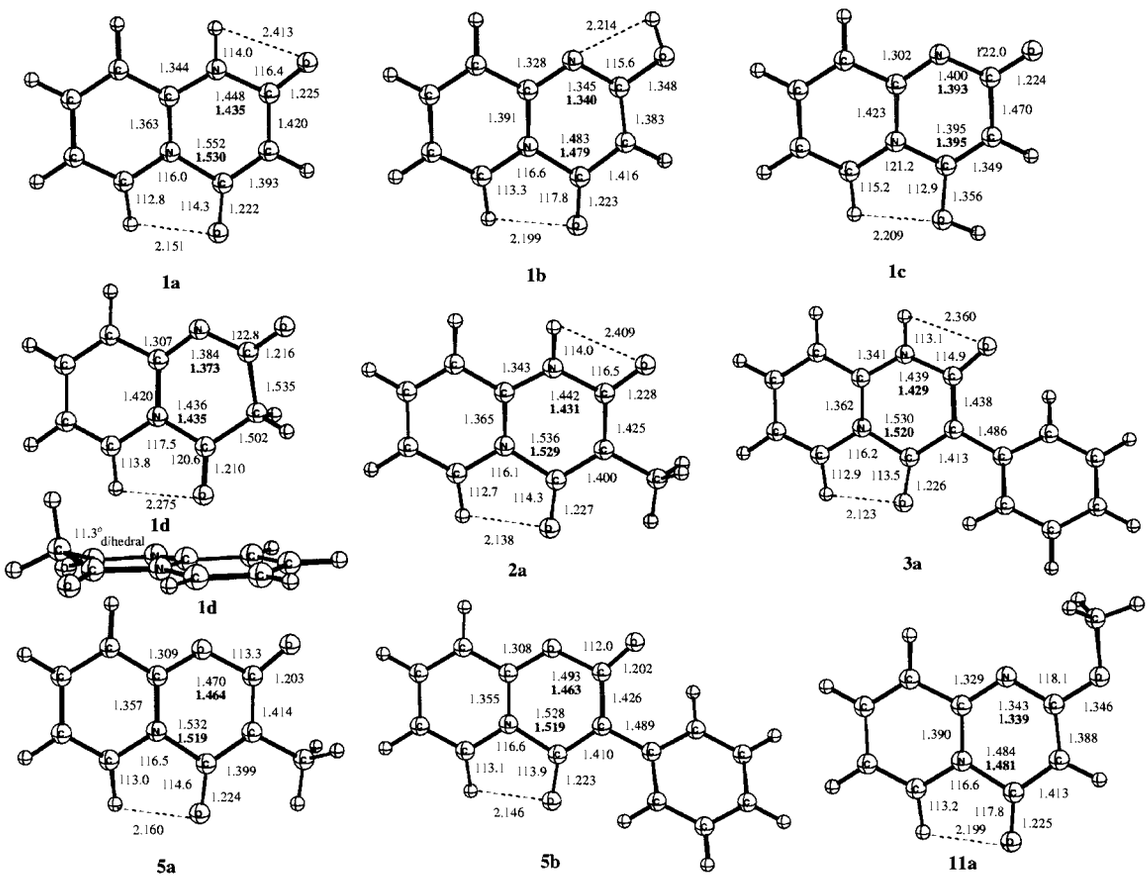

Chart 5 Calculated geometries (B3LYP/6-31G*; bond lengths in Å and bond angles in degrees). The SCRF values ($\varepsilon_r = 40$) are in bold.

Table 1 Selected bond lengths (Å) and angles (degree) determined by X-ray crystallography (the full data is given in the electronic supplementary information)

Compound 2a	
C4 N5	1.469(6)
O2 C2 N1	117.0(4)
O4 C4 N5	116.8(4)
Compound 3a[a]	
C4N5	1.4903(13)
O2 C2 N1	116.22(9)
O4 C4 N5	114.63(9)
N5 C6 H6	114.6(9)
Compound 5a[b]	
C4A N5A	1.487(8)
O2A C2A O1A	113.9(6)
O4A C4A N5A	115.6(6)
Compound 5b[a]	
C4 N5	1.487(3)
O2 C2 O1	112.8(2)
O4 C4 N5	114.6(2)
Compound 11b[b]	
N1A C10 A	1.335(6)
N1A C2A	1.321(6)
C2A C3A	1.382(7)
C3A C4A	1.389(7)
C4A N5A	1.444(6)
N5A C10A	1.392(6)
N1A C2A O2A	117.8(5)
O4A C4A N5A	118.1(5)
Compound 11c	
N1 C10	1.324(2)
N1 C2	1.363(2)
C2 C3	1.379(2)
C3 C4	1.391(2)
C4 N5	1.446(2)
N5 C10	1.380(2)
N1 C2 N2	111.09(13)
O4 C4 N5	117.12(15)

[a] The dihedral angle between phenyl and pyrimidine rings in **3a** is 23.44(0.04)°. For **5b** it is 38.00(0.04)°. [b] There are two molecules, termed A and B, in the crystals of **5a** and **11b**. As they have very similar bond lengths and angles, only one of them is shown in Figs. 3 and 5. See the electronic supplementary information for further details.

CH···O bond is similar to that identified computationally in ketene–pyridine zwitterions and the C_3O_2–pyridine complex, where it is *ca.* 2.2 and 2.8 Å, respectively.[15] The H-bonding causes a shift to higher frequencies of the C–H stretching frequency, by *ca.* 10 cm^{-1} in the complex, and 97 cm^{-1} in the zwitterion. The corresponding calculated frequency shift for C(6)–H(6) in mesoion **1a** is 81 cm^{-1}. However, the CH···O bond does not appear to be the main reason for the tilting of the C=O groups, as it cannot explain the similar structures of sydnones and munchnones discussed below. Also, any steric effect of the phenyl group in **3a** can be discounted since the same distortion is observed in the published X-ray structures of the parent **1a**[5] as well as compounds **7**[16] and **8**.[17] A similar but less pronounced distortion can be seen in the related compound **9**.[18] A structure very similar to that in **3** is also present in the mesitylimine analog **10**, which we describe elsewhere.[19] Compounds **2a**, **3a**, and **5b** feature *inter*molecular H-bonds C(6)–H(6)···O(4) (*ca.* 3 Å), as well. The NH-mesoions **2a** and **3a** also feature conventional *inter*molecular H-bonds N(1)–H(1)···O(2) (1.8–1.9 Å). A table of inter- and intra-molecular H-bond lengths in the crystals of **2a**, **3a**, **5a**,**b** and **11b**,**c** and structures showing the intermolecular H-bonds in **2a** and **5b** are given in the supplementary data (Table S10 and Figs. S1–S3). Selected bond lengths and angles are given in Table 1.§ The X-ray structures of **11b**,**c** are shown in Figs. 5 and 6.

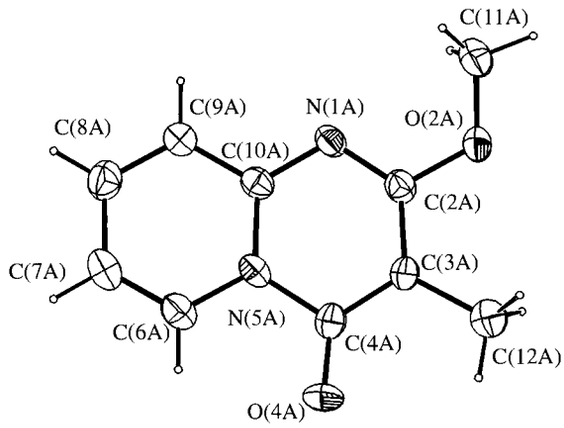

Fig. 5 ORTEP diagram of **11b**.

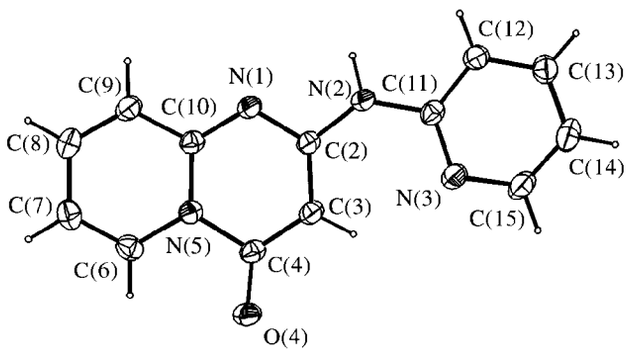

Fig. 6 ORTEP diagram of **11c**.

Enols of the types **1b** and **2b** cannot usually be isolated (except by matrix isolation, see below). For comparison, we have therefore determined the structures of the analogs **11b**,**c**. A few such compounds, **13** and **14**, are known to exist in the OH forms in the crystal when the enols are stabilised by intramolecular O···H bonding.[20,21] Compounds **11b**,**c**, **13**, and **14** show similar characteristics, with tilting of the C(4)=O groups towards 5-N (∠NCO = *ca.* 117°), tilting of C(2)–X towards N(1) (∠NCX = 111–118°), and elongation of the N(5)–CO bond (1.45 Å). Thus, these compounds show distortion similar to that in the mesoions **1a**, **2a**, **3**–**5**, *etc.*, but not quite so severely. The bond localisation implied in structures **11b**,**c**, **13**, and **14** as drawn does not represent the actual structures precisely; a significant contribution by the canonical structure **12** is indicated by the elongation of C(2)–C(3) to 1.38 Å, and the shortening of N(1)–C(2) to 1.36 Å in **11b**,**c**. Thus, the electronic structures of mesoions of type **1a** and pyridopyrimidinones of type **1b** appear to have much in common. This is borne out by the natural bond orbital (NBO) charges discussed in the theory section and by the calculated structures for **1a**–**d** (Chart 5). These calculated structures show long C(2)–C(3) and C(4)–N(5) bonds for **1a**, as in structure **17**. For **1b**, N(1)–C(2) is shortened and C(2)–C(3) lengthened in agreement with the resonance structures **11** ↔ **12**. For **1c** and **1d**, in contrast, the bond-localised structures drawn in Chart 1 correctly represent the molecules. The calculated C=O double bond lengths are nearly identical in **1a**–**d** at *ca.* 1.22 Å. The experimental C=O bond lengths in **2a**, **3a**, **5a**,**b** and **10** are always *ca.* 1.23 Å, and 1.22–1.25 Å for **11b**,**c** and **13**.

Some 4-quinolones show comparatively normal geometries around the carbonyl groups and C=O bond lengths of 1.23–

§ CCDC reference number 188/266. See http://www.rsc.org/suppdata/p2/b0/b003933k/ for crystallographic files in .cif format.

1.26 Å,[22] but 2-pyridones, especially of the isoquinolinone type, can show pronounced tilting of the C=O groups, as discussed in the theory section and shown in Chart 7.

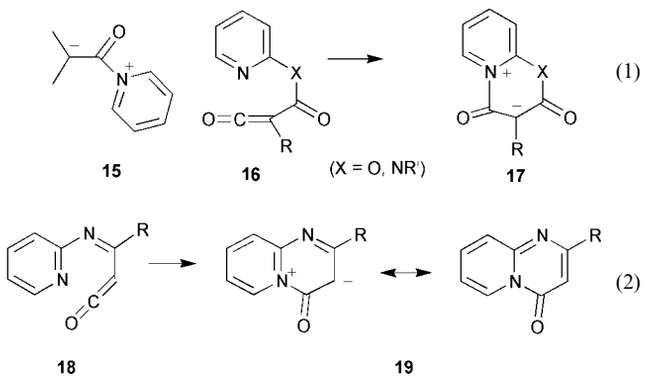

IR spectra

Mesoions and enols. We have reported the observation of ketene–pyridine zwitterions of type **15**, whose carbonyl groups give rise to absorptions in the region of *ca.* 1665–1685 cm^{-1} in the Ar matrix IR spectra.[23] This is lower than the calculated values for the gas phase ($\varepsilon_r = 1$) using the B3LYP/6-31G* method, and it is necessary to apply a polar solvent field effect in the calculations ($\varepsilon_r = 40$) in order to get good agreement with experiment. This also applies to the pyrrolopyridinyliumolates **6** in Ar matrices.[13] In the case of **6**, even lower values for the C=O stretching vibration are found in the experimental IR spectra in KBr.[13] Similar observations can be made for the mesoions **2** and **3**–**5**. Compound **4b** has IR absorptions in the Ar matrix at 1715m and 1666vs cm^{-1}. The B3LYP/6-31G* values for $\varepsilon_r = 1$ ($\varepsilon_r = 40$ in parentheses) are 1734, 1688 (1718, 1662) cm^{-1} for the two strongest bands. The KBr spectrum has these bands at 1688s, 1629vs cm^{-1}. For **5a** the values are 1789m, 1717s cm^{-1} in the Ar matrix. The B3LYP/6-31G* values are 1807, 1738 (1770, 1714) cm^{-1} for $\varepsilon_r = 1$ and 40, respectively, for the strongest bands. The KBr values are 1732m, 1665s cm^{-1}. It is immediately clear that, due to the very high polarity of these compounds, standard KBr spectra are not very useful for obtaining structural information (dipole moments >8 debye, see theory section). Even the Ar matrix isolated species do not behave as discrete gas phase molecules but experience a strong dielectric field. The highest wavenumber in **4b** is attributed to the C=O group at 4-C, and the matrix value is considerably higher than for normal amides or lactams (1650–1700 cm^{-1}). The lower wavenumber for **4b** at *ca.* 1665 cm^{-1} range is due to the C=O group at 2-C, and this value is normal for six-membered ring lactams. In agreement with the X-ray data, there is no indication of strong delocalisation of negative charge to weaken the double bond character of the C=O bonds. One can think of these molecules in terms of intramolecular trapping of a ketene by a pyridine to form a ketene–pyridine zwitterion (**16** → **17**). The mesoions so formed retain a long "pyridinylium" N–CO single bond. This results in a distorted six-membered ring as illustrated in an exaggerated way in structure **17**. Similar structural features are also seen in the quaternary pyrazolyliumolates formally resulting from ring closure of *N,N*-disubstituted hydrazones or imidoylhydrazines onto the central carbon atom of a ketene. The resulting intramolecular ammonium–CO single bonds are of the order of 1.56–1.62 Å, whereas the C=O bonds are normal, *ca.* 1.23 Å.[24] By analogy, the highly polar but non-mesoionic compound of type **19** can be thought of as the result of cyclisation of pyridyliminoketenes of type **18** [see eqns. (1) and (2)].

In the case of the NH-compounds **1** and **2**, there are further possibilities of tautomerism. Different tautomers can be present in solution and in the gas phase and hence also in the materials isolated in Ar matrices. In fact, the IR spectrum of **1** in an Ar matrix is totally different from that in KBr. The Ar matrix spectrum is in better agreement with calculations (B3LYP/6-31G*) for **1b** than for **1a** or **1c**. Compounds **1** and **2** show strong, sharp bands at 3570 and 3578 cm^{-1}, respectively, in the Ar matrix IR spectra, which can be ascribed to the OH forms (**1b**, **2b**) (Figs. 7 and 8). The calculated OH stretch is *ca.* 3555 cm^{-1}. The NH stretch in **1a** and **2a** is calculated at *ca.* 3465 cm^{-1} (B3LYP/6-31G*), and it is most unlikely that the experimental frequencies would be *ca.* 100 wavenumbers *higher* than the calculated ones in this region. The B3LYP/6-31G* calculated spectra allow a clear differentiation: the species present in matrices of **1** and **2** are clearly the non-mesoionic OH-forms **1b** and **2b** (Figs. 7 and 8). Furthermore, the Ar matrix IR spectra of **1** and **11a** (C=O stretch at 1729 and 1724 cm^{-1}, respectively) are very similar, as are those of **2** and **11b** (C=O stretch at 1701 cm^{-1} in both compounds; Fig. 9). Thus, non-mesoionic forms like **1b** and **2b** dominate in noble gas matrices. The forms **1c** and **1d** are never present to any significant extent under the conditions we have investigated here, but a thermal reaction to be reported elsewhere indicates that tautomer **1d** can be populated on gas phase thermolysis.[6]

As mentioned above, the B3LYP calculations with $\varepsilon_r = 40$ give good agreement with experimental IR spectra for the

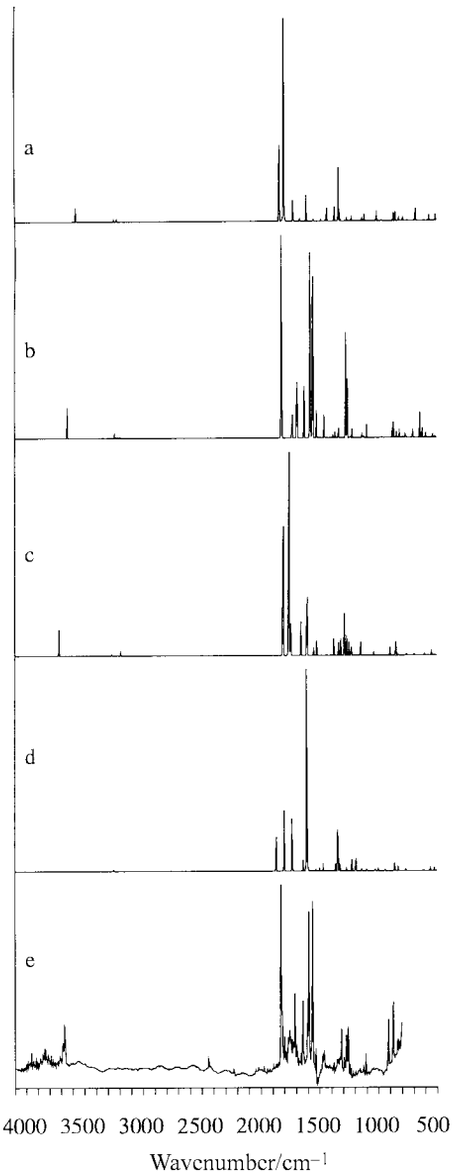

Fig. 7 IR spectra of **1**, (a) calcd. for **1a**, (b) calcd. for **1b**, (c) calcd. for **1c**, (d) calcd. for **1d**, (e) experimental Ar matrix. All calculations for $\varepsilon_r = 40$, B3LYP/6-31G*.

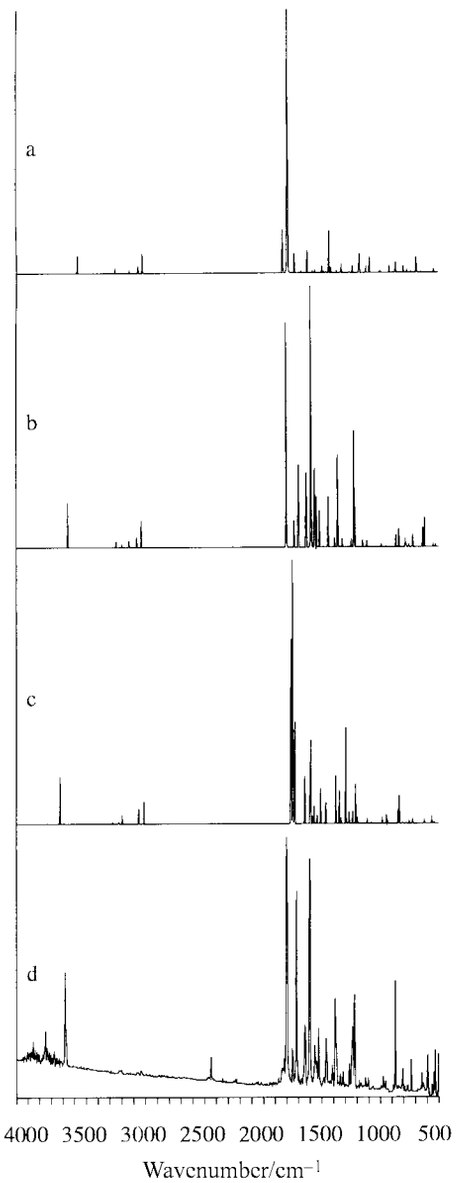

Fig. 8 IR spectra of **2**, (a) calcd. for **2a**, (b) calcd. for **2b**, (c) calcd. for **2c**, (d) experimental Ar matrix. All calculations for $\varepsilon_r = 40$, B3LYP/6-31G*.

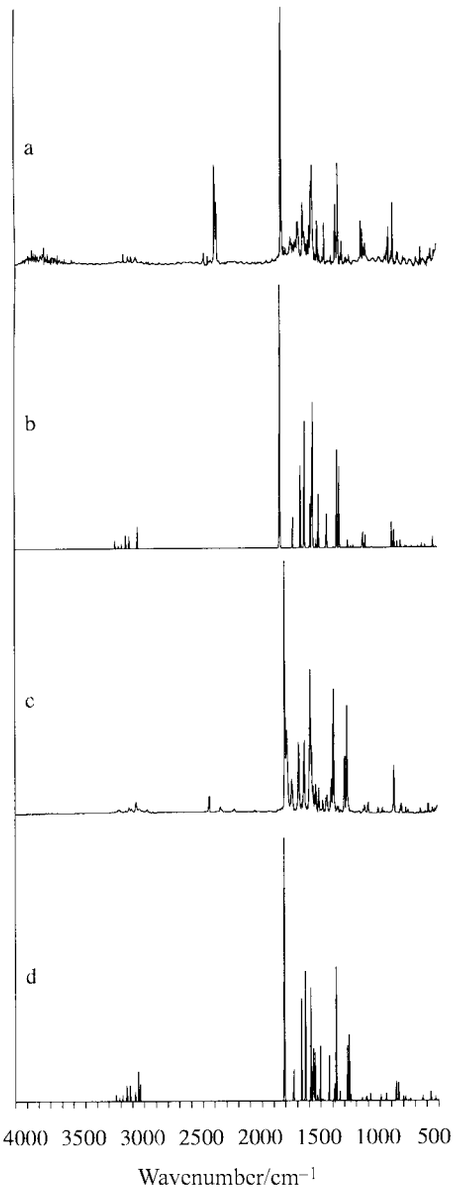

Fig. 9 IR spectra of (a) **11a** in Ar matrix, (b) calcd. for **11a**, (c) **11b** in Ar matrix, (d) calcd. for **11b**. All calculations for $\varepsilon_r = 1$, B3LYP/6-31G*. The peaks at 2270–2290 cm^{-1} in spectrum (a) are due to a small amount of C_3O_2 formed by thermolysis.

matrix isolated mesoions **4a** and **4b**, which, because of the *N*-methyl groups, cannot exist in any other tautomeric forms (spectra of **4a** shown in Fig. 10). However, for the same compound **4a** in KBr, the C=O stretches are found *ca.* 40 wavenumbers lower, and this is not accounted for properly in a B3LYP calculation with the 6-31G* basis set (60 cm^{-1} too high for $\varepsilon_r = 1$, and 40 cm^{-1} too high for $\varepsilon_r = 40$). The addition of diffuse functions using the 6-31+G* basis set improves the agreement, bringing the C=O stretches down to the correct wavenumbers [still 30 cm^{-1} too high for $\varepsilon_r = 1$, but correct at 1697, 1646 cm^{-1} for $\varepsilon_r = 40$ (see also Theory section and Table 3)]. The latter basis set also provides good agreement with the experimental C=O stretch wavenumbers in KBr for the NH mesoions **1a** and **2a**. However, there is poor overall agreement between calculated and experimental spectra in the fingerprint region. The reason is presumably that these highly polar compounds do not exist as discrete molecules in the crystal (spectra in KBr) but as H-bonded aggregates, as indicated by the strong and broad bands between 2000 and 3000 cm^{-1} as already noted by Katritzky and Waring.[3a] The X-ray crystal structures of **2a** and **3a** reveal *inter*molecular H-bonds N(1)–H(1)···O(2), as do those of **2a**, **3a**, and **5b** at C(6)–H(6)···O(4) (see X-ray structures section and supplementary data). The IR spectra in KBr are listed in the Experimental section, and the calculated spectra are tabulated in the supplementary data.

Comparison with five-membered ring mesoions. C=O tilting and ketene resonance structures

So what is the reason for the tilted C=O structures? Similar structures around the carbonyl groups are found in the sydnones **20**[25] and munchnones **22**,[26] with OCO angles of *ca.* 121° (contrasting CCO at *ca.* 138°) and endocyclic C–O bond lengths of the order of 1.40 Å (Chart 6). This has been interpreted in terms of a "no bond resonance" with the open chain ketene type structures **21** and **23**,[25a,b] whereby it should be kept in mind that IR spectroscopy clearly reveals that the compounds are cyclic ketones. The carbonyl groups typically absorb in the range 1730–1795 cm^{-1} in the KBr spectra, which is normal for five-membered ring lactones, thus indicating that there is certainly not a great deal of enolate character. However, here too, we find a significant shift to higher wavenumbers in the Ar matrix isolated molecules, *e.g.* from 1765 to 1804 or from 1794 to 1825 for the munchnones **24** and **25**, respectively.[27] These high values are in agreement with some contribution

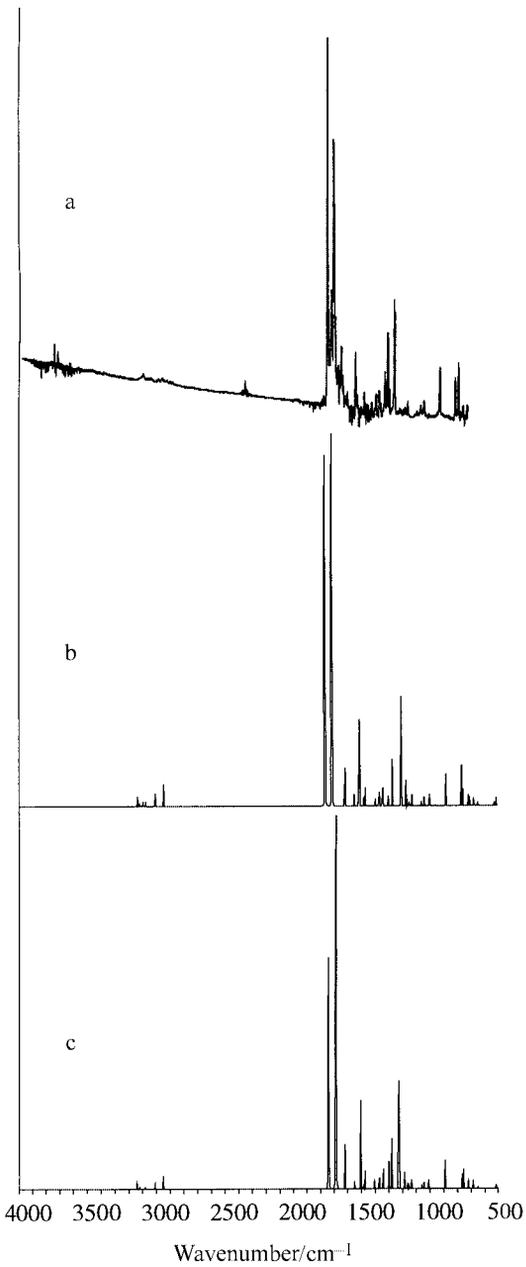

Fig. 10 IR spectra of **4a**, (a) in Ar matrix, (b) calcd. for **4a**, $\varepsilon_r = 1$, (c) calcd. for **4a**, $\varepsilon_r = 40$ (B3LYP/6-31G*).

from ketene canonical structures. The subject is elaborated further in the Theory section.

There has been much discussion in the literature about the possible *valence isomerisation* of sydnones and munchnones to the open-chain ketene forms,[28] but although some circumstantial evidence has been produced, no concrete evidence exists, and there is no convincing report of the observation of ring-opened ketenes of types **21** or **23**. There are only two authenticated cases of direct observation of valence isomerisation between five-membered mesoionic compounds and open-chain ketene structures, namely those of 1,3,2-oxathiazolylium-5-olate (**26** → **27**)[29] and 1-oxopyrrolo[1,2-*a*]pyridin-4-ylium-3-olate **6**[13] whose ketene valence isomers have been observed by low temperature matrix isolation IR spectroscopy.[30]

Theory

Density functional calculations were carried out using the Gaussian 98 series of programs.[31] Full geometry optimisations were carried out with the B3LYP method,[32] using the split-valence polarised 6-31G* basis set. Higher-level relative energies were obtained through B3LYP/6-311+G** calculations, including zero-point energy (ZPE) correction. The effect of a dielectric medium was examined using self-consistent reaction field (SCRF) methods; geometry optimisations and vibrational frequency computations were carried out using the Onsager method,[33] while high-level single-point energy calculations were obtained through the SCIPCM theory.[31,34] NMR chemical shift calculations were performed using the gauge-independent atomic orbital (GIAO) method.[35] Infrared spectra were computed at the B3LYP/6-31G* and B3LYP/6-31+G* levels and the directly calculated frequencies were scaled by a factor of 0.9613.[36] Charge density analysis was carried out using the natural bond orbital (NBO) approach.[37]

Table 2 Calculated relative energies[a] (kJ mol^{-1}) and dipole moments[b] (debye) of **1a–d** and **2a–c**

	1		**2**	
Species	$\varepsilon_r = 1$	$\varepsilon_r = 40$	$\varepsilon_r = 1$	$\varepsilon_r = 40$
a	0.0 (8.33)	0.0 (11.34)	0.0 (7.95)	0.0 (10.90)
b	−17.9 (4.68)	8.6 (6.18)	−19.5 (4.20)	5.9 (5.58)
c	66.8 (7.52)	63.0 (9.82)	61.3 (7.10)	62.7 (9.28)
d	55.8 (5.84)	43.4 (8.27)		

[a] B3LYP/6-311+G**//B3LYP/6-31G* + ZPE level. [b] Dipole moments (B3LYP/6-31G*) are in parentheses.

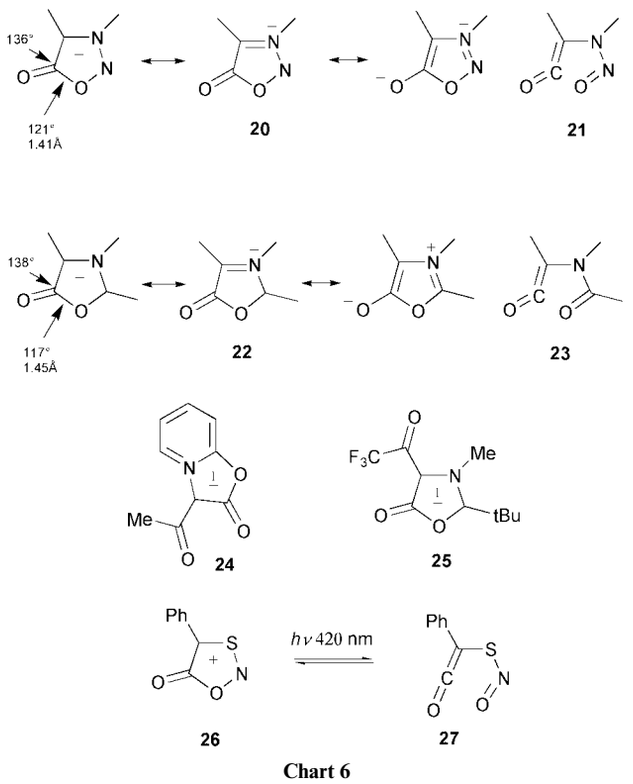

Chart 6

First, we examine the tautomeric equilibria between the mesoions (**a**) and the OH tautomers (**b**) of compounds **1** and **2** in the gas phase ($\varepsilon_r = 1$) and in a polar medium ($\varepsilon_r = 40$) (Table 2). For the parent compounds (**1a** and **1b**), the OH tautomer is preferred in the gas phase (by 18 kJ mol^{-1}). The mesoion **1a** is calculated to have a very large dipole moment of 8.33 debye ($\varepsilon_r = 1$), almost twice that calculated for **1b** (Table 2). Thus, **1a** is expected to be strongly stabilised in a polarisable dielectric medium. The large differential stabilisation effect results in a reversal of the tautomeric equilibrium in the condensed phase. In a dielectric medium of $\varepsilon_r = 40$, **1a** is predicted to be more stable than **1b** by 9 kJ mol^{-1}. As with the parent analogues, the OH tautomer **2b** is favored over the mesoion **2a** (by 20 kJ

mol^{-1}) in the gas phase. Here too, the medium effect leads to a reversal of the **2a**–**2b** tautomeric equilibrium on going from the gas phase to a polar medium. The calculated medium effects on the NH–OH tautomerism of compounds **1** and **2** are in excellent accord with the experimental NMR and IR findings. We have also calculated the energies of the two other possible tautomers (**c** and **d** for **1**, **c** for **2**), and they lie significantly higher in energy (Table 2).

All mesoions are characterized by long C–N bonds (1.442–1.552 Å) and tilting of the C=O groups (∠NCO = 112–116°) (Chart 5). The C–N bonds are shortened by 0.1–0.2 Å in a polar environment ($\varepsilon_r = 40$). NBO charge density analysis reveals a strong charge alternation in the pyrimidine ring. For instance, mesoion **1a** is characterised by strong negative charges at the N atoms (−0.40 and −0.61) and carbon 3-C (−0.52), while the carbonyl carbons (0.61 and 0.63) and 9a-C (0.46) carry a strong positive charge. Compared to 2-aminopyridine, there is a significant decrease in electron population at the N atoms (see the supplementary material). This suggests that there is localisation of positive charge at these atoms. The characteristic carbanion centre is located at the 3-C atom, which has a high field ^{13}C chemical shift. The NBO atomic charge at 3-C correlates reasonably well with the magnitude of the ^{13}C chemical shift for all the mesoions considered. It is worth noting that the Mulliken bond orders for the two CO–N bonds are low (0.628 and 0.800 in **1a**, HF/6-31G*) compared to that calculated for a normal C–N single bond (0.95 for methylamine and piperidine). As pointed out in the previous section, the C(4)=O stretching frequencies of the mesoionic compounds are significantly higher than those in lactams and lactones. All these structural, spectroscopic, and charge data thus confirm that the mesoionic compounds can be described as intramolecular ketene–pyridine zwitterions **17**. It is important to note that the non-mesoionic tautomers are also characterized by large dipole moments, >5 debye (Table 2). NBO analysis indicates that their charge distributions are similar to those of the mesoions (see the supplementary material). Thus, it is not surprising that the ^{13}C NMR chemical shifts of **1a** and **1b** are quite similar, and this confirms the strongly zwitterionic character of the enols **1b** and **2b** as in **12** and **19**.

Other compounds found in the literature show tilting of C=O groups, in particular the isoquinolinones **32**, **34**, **36**, for which potential ketene valence isomeric (or mesomeric) structures **33**, **35**, **37** can be written (Chart 7).[38] In order to shed light on the unusual tilting of the C=O groups in the mesoions, we have examined the structures of two prototypical systems, namely the mesoionic pyrimidinyliumolate **28** and 2-pyridone (**30**) (Chart 7). In both cases, one can draw potential open-chain ketene isomers (**29** and **31**, respectively). Partial optimizations (B3LYP/6-31G*) were carried out for a series of fixed C–N bond lengths (1.20–1.80 Å). The correlation between the CO–N bond lengths and four other structural parameters, *r*(C=O), *r*(C–C), ∠NCO and ∠CCO, which characterise the ketene-type structure, are summarised in Figs. 11 and 12. For both **28** and **30**, there is an almost perfect correlation ($r^2 = 0.99$) between the CO–N bond length and the key ketene structural parameters. An increase of *r*(C–N) leads to a shortening of *r*(C=O) and *r*(C–C), a decrease of ∠NCO and an increase of ∠CCO. These changes clearly indicate an increasing contribution by the ketene resonance structures for long C–N bonds. Note also that the tilting of the ylide C=O group correlates with an increased C=O stretching frequency.

IR spectra calculated at the B3LYP/6-31G* level are generally in good agreement with experiment. However, for the strongly polar mesoionic compounds, several vibrational modes may be expected to undergo solvent shifts in a polar medium. The C=O stretching frequencies are red shifted by 20–30 cm^{-1} on going from the gas phase to a dielectric medium of $\varepsilon_r = 40$ (Table 3). Thus, a better agreement between theory and experiment is achieved using the SCRF calculated

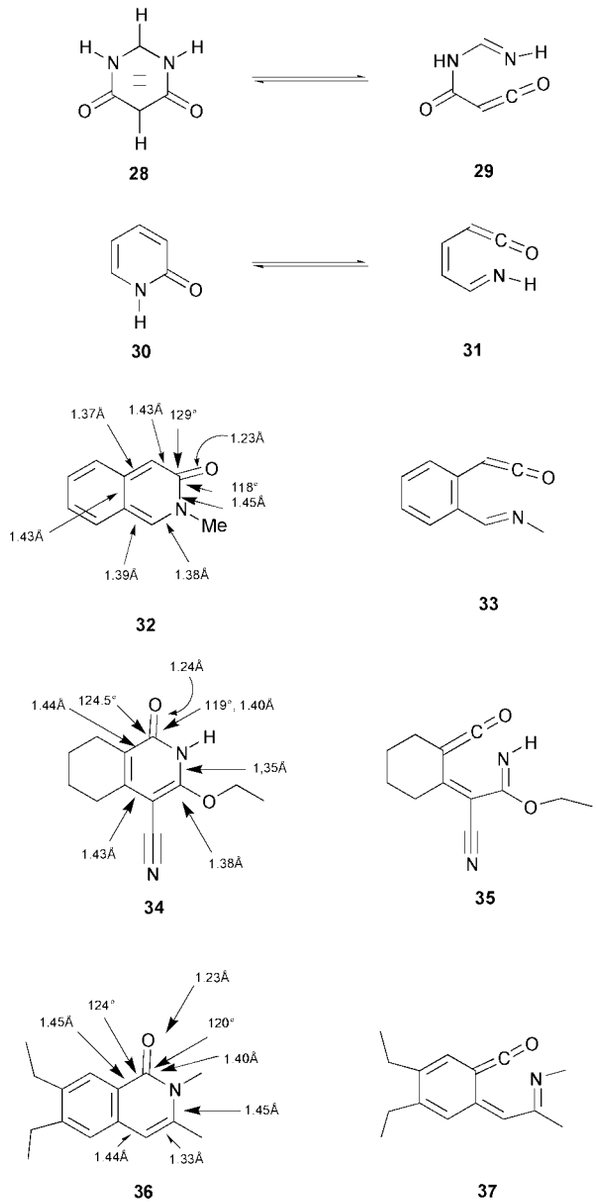

Chart 7 Potential ring opening equilibria and structures of isoquinolinones.

frequencies. However, the SCRF calculated C=O frequencies of the mesoions are still somewhat high compared to the experimental values in KBr. It is well established that diffuse functions are particularly important for prediction of solvent shifts using Onsager's reaction field model.[33b] Hence, it is instructive to consider also the use of the 6-31+G* basis set. For the parent mesoion **1a**, there are small differences between the B3LYP/6-31G* and B3LYP/6-31+G* IR spectra (see the supplementary material) except for the C=O stretching vibrations. For these C=O frequencies, inclusion of diffuse functions on heavy atoms (6-31+G*) leads to a significant lowering of the wavenumbers, by 42 and 54 cm^{-1} (Table 3). The calculated B3LYP/6-31+G* values are in pleasing agreement with experiment. A similarly good agreement is obtained for other mesoionic compounds **2a**, **4a**, **4b** and **5a** (Table 3).

The relative energies of mesoions and the potential open-chain ketene *valence isomers* **16** (X = NH or O; R = H, eqn. (1)) are presented in Table 4. The cyclic mesoions are substantially more stable than the corresponding ketene isomers in both cases. Due to the greater stabilisation of the more polar mesoionic structures, the preference for the mesoions is further increased in polar media ($\varepsilon_r = 40$). The strong preference for the

Table 3 Calculated C=O stretching frequencies[a] (cm^{-1}) of mesoionic compounds

	$\varepsilon_r = 1$			$\varepsilon_r = 40$		
Species	6-31G*	6-31+G*	Expt.	6-31G*	6-31+G*	Expt.
1a	1764, 1732	1730, 1692		1739, 1700	1697, 1646	1690, 1652
2a	1735, 1709	1702, 1669		1721, 1681	1684, 1635	1701, 1658
4a	1765, 1715	1729, 1697	1739, 1711	1740, 1685	1697, 1637	1703, 1652
4b	1734, 1688	1718, 1662	1715, 1666	1718, 1662	1681, 1616	1688, 1629
5a	1807, 1738	1773, 1704	1789, 1717	1770, 1714	1730, 1665	1732, 1665

[a] B3LYP level, scaled by 0.9613 (ref. 34).

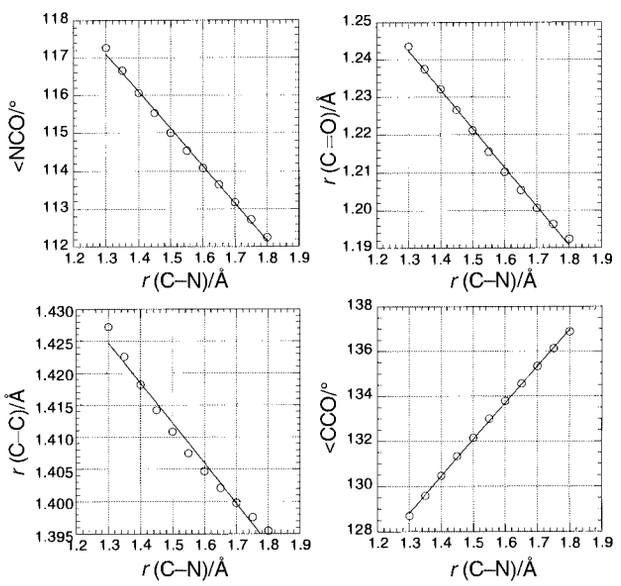

Fig. 11 Correlation of ∠NCO *versus* *r*(C–N), *r*(C=O) *versus* *r*(C–N), *r*(C–C) *versus* *r*(C–N), and ∠CCO *versus* *r*(C–N) in mesoionic pyrimidinyliumolates **28**.

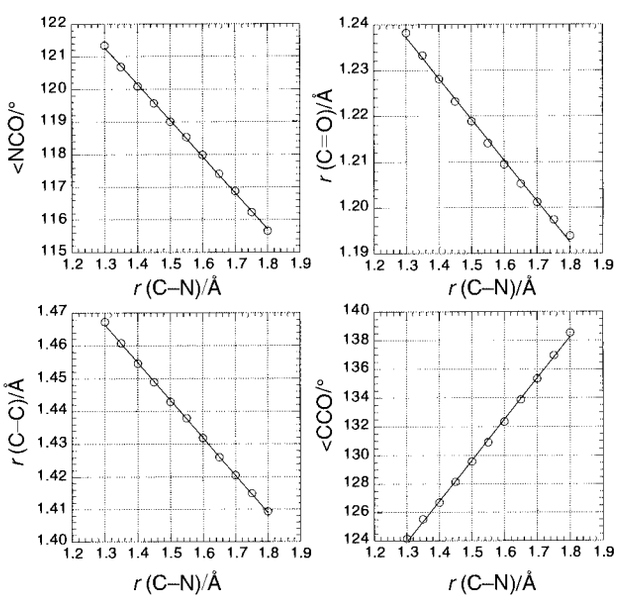

Fig. 12 Correlation of ∠NCO *versus* *r*(C–N), *r*(C=O) *versus* *r*(C–N), *r*(C–C) *versus* *r*(C–N), and ∠CCO *versus* *r*(C–N) in 2-pyridone **30**.

cyclic mesoions helps explain the difficulty of observing the open-chain ketene valence isomers of type **16**.[6]

Conclusion

Pyridopyrimidinones of type **1** and **2** exist in the crystalline and solution phases as mesoions **1a** and **2a**. However, the OH-tautomers **1b** and **2b** are of lower energy in the gas phase and these are the tautomers isolated in Ar matrices. Not only the mesoionic compounds of type **1a**, but also the "enols" of type **1b** are highly polarised, zwitterionic compounds. The structures of all mesoionic compounds of these and related types, including sydnones and munchnones, tend to exhibit strong tilting of the carbonyl oxygens towards the neighbouring "lactam" nitrogens or "lactone" oxygens as well as strong elongation of the "lactam" bonds (C(4)–N(5) = *ca.* 1.49 Å). In agreement with previous investigations,[2] the structures and spectroscopic data indicate localisation of charges in a positive pyridinium and a negative malonyl fragment as in formula **17**. The structures of OH-tautomers of the type **1b**, **2b** and **11** likewise show pronounced zwitterionic character, as in the resonance form **12**. The molecules **17** and **19** can be thought of as arising from intramolecular zwitterion formation between a ketene and a pyridine: **16** → **17** and **18** → **19** [eqns. (1) and (2)].

Table 4 Calculated relative energies[a] (kJ mol^{-1}) of ketene valence isomers **16** and mesoions **17**

	X = NH, R = H		X = O, R = H	
Species	$\varepsilon_r = 1$	$\varepsilon_r = 40$	$\varepsilon_r = 1$	$\varepsilon_r = 40$
Mesoion **17**	0.0	0.0	0.0	0.0
s-*trans* Ketene **16**	64.3	92.2	34.0	52.8
s-*cis* Ketene **16**	41.5	70.5	36.9	56.1

[a] B3LYP/6-311+G**//B3LYP/6-31G* + ZPE level.

Experimental

General

Infrared spectra were recorded on Perkin-Elmer 1700X or System 2000 FT-IR spectrometers. Ar matrix IR spectra were obtained at 7–14 K using an Air Products CSW-202-6.5 closed cycle He cryostat with BaF_2 or KBr windows. UV spectra were measured on a Shimadzu UV-1601 spectrometer, and mass spectra on a Kratos MS25RFA spectrometer (EI, 70 eV). NMR spectra were recorded on a Bruker AX 200 spectrometer (200.13 MHz for ^1H and 50.34 MHz for ^{13}C unless indicated otherwise) with $SiMe_4$ as internal standard. *J* Values are given in Hz. Dichloromethane was dried over CaH_2 and was freshly distilled before use. Methanol was distilled from magnesium. All other chemicals were used in the commercially available quality.

Crystallography

Cell constants for compounds **2a**, **5a**, **5b**, **11b** and **11c** were determined by a least-squares fit to the setting parameters of 25 independent reflections measured on an Enraf-Nonius CAD4 four circle diffractometer employing graphite monochromated Mo-Kα radiation (0.71073 Å). For compound **3** data were collected on a Siemens SMART CCD diffractometer. Data reduction and empirical absorption corrections were performed with the XTAL[39] package, except for **2a**, which was not

corrected for absorption and compound **3** for which data reduction was performed with the SHELXTL system. Crystal data are given in Table 5.

Structure solutions. Structures were solved by direct methods with SHELXS-86[40] and refined by full-matrix least-squares analysis with SHELXL-97.[41] All non-H atoms were refined with anisotropic thermal parameters. The atomic nomenclature is defined in Figs. 1–6 drawn with PLATON.[42]

2-Oxo-1,2-dihydro-5λ^5-pyrido[1,2-*a*]pyrimidin-5-ylium-4-olate 1

Compound **1** was prepared according to Tschitschibabin;[1] ν_{max}(KBr, largely form **1a**)/cm^{-1} 3400vbr, 3096m, 2600vbr, 1690s, 1652s, 1616s, 1592m–s, 1524m, 1484w, 1434w, 1365m–s, 1332m–s, 1282m, 1259w, 1134w, 1062vw, 1031m, 983w, 939w, 897m, 774m, 755w, 735w, 772w, 666w–m, 555w, 540w, 510m–s, 452m–s, 419w; ν_{max}(Ar, 14 K, largely form **1b**)/cm^{-1} 3570m, 1729s, 1611m, 1543m, 1506w, 1492s, 1460s, 1433w, 1215m, 1174w, 1157m, 1006w, 815m, 773m; δ_H(DMSO-d_6) 12.04 (s, 1H), 8.92 (d, ^3J 7, 1H, 6-H), 8.07 (dd, $^3J_1$ 7, $^3J_2$ 8, 1H, 8-H), 7.41 (d, J 8, 2H, 9-H), 7.31 (t, J 7, 1H, 7-H), 4.96 (s, 1H, 3-H); δ_H(MeOH-d_4) 9.07 (d, 1H), 8.14 (t, 1H), 7.48 (d, 1H), 7.40 (t, 1H), 5.23 (s, 1H). The ^{13}C NMR spectra were obtained in DMSO-d_6 solution at room temperature (25000 scans) or better at 80 °C (3000 scans): δ_C(DMSO-d_6, 125.8 MHz, 29 °C) 163.2 (s), 156.1 (s), 148.0 (s), 141.4 (8-C), 128.8 (6-C), 118.0 (br, weak at RT, 9-C), 115.6 (7-C), 81.6 (3-C). The NMR assignments are supported by a 2D ^{1}H–^{13}C HSQC correlation run in DMSO-d_6 at 80 °C.

General procedure for the synthesis of pyrimidinyliumolates from malonic acids

The appropriate 2-substituted malonic acid (10 mmol) was dissolved in 10 ml of dichloromethane, treated with PCl_5 (25 mmol) and stirred for 2 h under exclusion of moisture. Dissolved HCl gas was removed by pumping at *ca.* 200 mbar for 10 min. A solution of the requisite pyridine derivative (10 mmol) in dichloromethane was added dropwise with stirring. The coloured precipitate was filtered after *ca.* 30 min and purified by sublimation and/or recrystallization. The following compounds were prepared in this manner.

3-Methyl-2-oxo-1,2-dihydro-5λ^5-pyrido[1,2-*a*]pyrimidin-5-ylium-4-olate 2a. Compound **2a** was obtained as yellow crystals in 78% yield. It has been prepared previously using the "magic malonate" method;[43] ν_{max}(KBr, form **2a**)/cm^{-1} 3500br, 1701vs, 1658s, 1653s, 1520s, 1224s, 1989w, 874m, 797s, 703m, 570w, 530w; ν_{max}(Ar, 7 K, form **2b**)/cm^{-1} 3578s, 1700s, 1696s, 1615s, 1505s, 1500s, 1283m, 1119m, 770m; δ_H($CDCl_3$, 500.13 MHz) 13.8 (1H, br), 8.9 (d, J 7, 1H, 6-H), 8.0 (t, J 8, 1H, 8-H), 7.4 (d, J 8, 1H, 9-H), 7.3 (t, J 7, 1H, 7-H), 1.87 (s, 3H, CH_3); δ_C($CDCl_3$, 125.8 MHz) 162.1 (s, 2-C), 155.9 (s, 4-C), 146.2 (s, 9a-C), 139.8 (8-C), 128.4 (6-C), 117.6 (br, weak, 9-C), 115.3 (7-C), 89.5 (3-C), 9.4 (q, CH_3). The NMR assignments are supported by a 2D HSQC spectrum.

A crystal from DMSO-d_6 solution was covered with silicone grease without removal of the solvent and mounted on the X-ray diffractometer.

3-Phenyl-2-oxo-1,2-dihydro-5λ^5-pyrido[1,2-*a*]pyrimidin-5-ylium-4-olate 3a. The compound was obtained as yellow crystals in 68% yield after sublimation at 180 °C (0.5 mbar); mp 300–305 °C (lit.[43] 305–306 °C; yield 73% by the "magic malonate" method); δ_H(500.13 MHz, DMSO-d_6) 12.34 (1H, br), 9.04 (d, 1H, 6-H), 8.10 (d, 1H, 8-H), 7.68–7.69 (2H, arom. *ortho*), 7.41 (d, 1H, 9-H), 7.35 (t, 1H, 7-H), 7.29 (t, 2H, arom. *meta*), 7.13 (t, 1H, arom. *para*); δ_C(125.8 MHz, $CDCl_3$) 160.3 (s, CO), 154.7 (s, CO), 146.2 (s, 9a-C), 141.8 (8-C), 134.9 (s, 1′-C), 130.5 (d, arom. *ortho*), 129.3 (6-C), 127.0 (d, arom. *meta*), 125.3 (d, arom. *para*), 115.87 and 115.81 (d, 9-C and 7-C), 94.3 (s, 3-C). The NMR assignments are supported by a 2D HSQC spectrum recorded from $CDCl_3$ solution. Anal. Calcd for $C_{14}H_{10}N_2O_2$: C, 70.56; H, 4.23; N, 11.77. Found: C, 70.75; H, 4.25; N, 11.61%.

Single crystals of **3** were obtained by slow evaporation from DMSO solution; a crystal was selected without removal of the solvent, mounted in Paratone oil, and immediately transferred to the cold gas stream of the X-ray diffractometer.

1-Methyl-2-oxo-1,2-dihydro-5λ^5-pyrido[1,2-*a*]pyrimidin-5-ylium-4-olate 4a

The compound was prepared by the method of Potts and Sorm;[9] mp 244–246 °C (lit.[9] 243–245 °C); ν_{max}(KBr)/cm^{-1} 3109w, 3019w, 1703s, 1652s, 1631m, 1599w, 1518w, 1322m, 1297m, 1269m, 922w, 783m and 775m; ν_{max}(Ar, 7 K)/cm^{-1} 1739s, 1711m, 1693s, 1658w, 1637w, 1532w, 1488vw, 1356vw, 1313vw, 1294m, 1243m, 907w, 793w, 769w; δ_H($CDCl_3$) 9.37 (dd, ^3J 7.1, ^4J 1.0, 1H, 6-H), 8.10 (ddd, $^3J_1$ 8.7, $^3J_2$ 7.1, ^4J 1.0, 1H, 8-H), 7.47 (ddd, ^3J 8.7, ^4J ^5J 1.0, 1H, 9-H), 7.34 (ddd, $^3J_1$ $^3J_2$ 7.1, ^4J 1.0, 1H, 7-H), 5.40 (s, 1H, 3-H), 3.71 (s, 3H, Me).

1,3-Dimethyl-2-oxo-1,2-dihydro-5λ^5-pyrido[1,2-*a*]pyrimidin-5-ylium-4-olate 4b

The crude product was purified by sublimation (1 mbar, 150 °C) and recrystallisation from ethanol to yield 1.48 g (78%) of bright yellow needles, mp 250–252 °C; ν_{max}(KBr)/cm^{-1} 1688s, 1629vs, 1600m, 1559m, 1517m, 1388m, 1374w, 1339m, 1307m, 1279m–w, 1210m–w, 1158m, 1094m, 983m, 778m, 751m, 699w, 445w, 415m; ν_{max}(Ar, 7 K)/cm^{-1} 1715m–s, 1666vs, 1640m, 1534w, 1443w, 1383w, 1343w, 1312w, 1209w, 1154w, 1088w, 1030vw, 970m, 766w, 752vw, 668w; λ_{max}(MeCN)/nm 236 (log (ε/dm^3 mol^{-1} cm^{-1}) 4.228), 247 (4.157), 277 (3.973), 320 (sh, 3.352), 334 (3.431), 374 (3.505); δ_H(DMSO-d_6) 9.16 (dd, ^3J 6.9, ^4J 1.0, 1H,6-H), 8.23 (ddd, $^3J_1$ 8.9, $^3J_2$ 7.0, ^4J 1.5, 1H, 8-H), 7.78 (d, ^3J 8.9, 9-H), 7.44 (ddd, $^3J_1$ 7.0, $^3J_2$ 6.9, ^4J 1.0, 1H, 7-H), 3.59 (s, 3H, N-Me), 1.87 (s, 3H, C-Me); δ_C(DMSO-d_6) 159.53 (s, CO), 153.55 (s, CO), 145.67 (s, 9a-C), 142.24 (d, 8-C), 130.25 (d, 6-C), 115.76 (d, 7-C), 114.35 (d, 9-C), 88.07 (s, 3-C), 29.49 (q, N-Me), 10.61 (q, C-Me); m/z 191 (M^+ + 1, 13%), 190 (M^+, 98), 162 (96) and 161 (100). Anal. Calcd for $C_{10}H_{10}N_2O_2$: C, 63.14; H, 5.30; N, 14.73. Found: C, 62.96; H, 5.32; N, 14.66%.

1-Methyl-3-phenyl-2-oxo-1,2-dihydro-5λ^5-pyrido[1,2-*a*]-pyrimidin-5-ylium-4-olate 4c

The compound was prepared in 55% yield according to the general procedure; yellow crystals, mp 193–194 °C; δ_H(CD_3OD) 9.38 (d, 1H, 6-H), 8.30 (t, 1H, 8-H), 7.89 (d, 1H, 9-H), 7.45 (t, 1H, 7-H), 7.58–7.20 (m, 5H arom.), 3.79 (s, 3H, Me); δ_C(DMSO-d_6) 161.5 (s), 156.0 (s), 148.0 (s), 144.6 (d), 135.4 (s), 132.3 (d), 132.2 (d, phenyl), 128.8 (d, phenyl), 127.6 (d), 117.7 (d), 115.6 (d), 98.2 (d), 30.8 (q). The NMR assignments given in Chart 2 are based on the B3LYP calculations; m/z 252.088764 (calcd 252.089329; 30%), 224 (100), 223 (85). Anal. Calcd for $C_{15}H_{12}N_2O_2$: C, 71.42; H, 4.79; N, 11.10. Found: C, 71.67; H, 4.73; N, 10.95%.

3-Methyl-2-oxo-5λ^5-pyrido[2,1-*b*][1,3]oxazin-5-ylium-4-olate 5a

The crude product was purified by sublimation (1 mbar, 145 °C) to yield 1.21 g (75%) of yellow crystals, mp 250–252 °C; ν_{max}(KBr)/cm^{-1} 3102w, 3067w, 1732m, 1665s, 1627s, 1565w, 1544w, 1497m, 1380w, 1333m, 1298m, 1129m, 1090m, 1039w, 975m, 908m, 801m, 792m, 755m, 724m, 702w, 684w, 660w, 537m; ν_{max}(Ar, 14 K)/cm^{-1} 1789m, 1776w, 1717s, 1711sh, 1694w, 1635w, 1503m, 1380vw, 1309w, 1285w, 892w, 778w, 743w; λ_{max}(MeCN)/nm 247 (log (ε/dm^3 mol^{-1} cm^{-1}) 4.403), 258sh (4.114), 285 (3.862), 313 (3.593), 327 (3.600), 357 (3.646); δ_H($CDCl_3$) 9.24 (dd, ^3J 7.0, ^4J 1.7, 1H, 6-H), 8.24 (ddd, $^3J_1$ $^3J_2$

Table 5 Crystal data

	2a	3a	5a	5b	11b	11c
Formula	$C_9H_8N_2O_2$	$C_{14}H_{10}N_2O_2$	$C_9H_7NO_3$	$C_{14}H_9NO_3$	$C_{10}H_{10}N_2O_2$	$C_{13}H_{10}N_4O$
M	176.17	238.24	177.16	239.22	190.20	238.25
Crystal system	Monoclinic	Triclinic	Monoclinic	Monoclinic	Monoclinic	Monoclinic
a/Å	9.116(6)	6.5287(1)	7.688(1)	7.318(2)	10.189(2)	10.868(3)
b/Å	5.066(1)	7.3004(1)	13.3074(9)	11.984(1)	15.928(3)	8.703(1)
c/Å	17.13(2)	12.0735(1)	15.144(3)	12.378(3)	11.200(3)	11.834(4)
α/°		98.260(1)				
β/°	93.97(3)	101.086(1)	93.243(9)	90.71(1)	94.683(8)	100.67(1)
γ/°		101.871(1)				
U/Å^3	789.2(1)	542.48(1)	1546.9(4)	1085.5(4)	1811.5(7)	1100.0(5)
T/K	295	203	295	295	295	295
Space group	$P2_1/n$ (No. 14)	$P\bar{1}$ (No. 2)	$P2_1/c$ (No. 14)	$P2_1/n$ (No. 14)	$P2_1/n$ (No. 14)	$P2_1/c$ (No. 14)
Z	4	2	8	4	8	4
μ/cm^{-1}	1.08	1.00	1.16	1.05	1.00	0.97
N (R_{int})	1380 (0.0402)	2396 (0.0134)	2712 (0.0703)	1909 (0.0296)	3189 (0.1082)	1929 (0.0285)
R (obs. data)	0.0496	0.0360	0.0599	0.0377	0.0514	0.0374
wR_2 (all data)	0.1880	0.1062	0.1920	0.1184	0.1680	0.1083

7.0, ^4J 1.7, 1H, 8-H), 7.55 (t, 1H, 7-H), 7.52 (d, 1H, 9-H), 2.05 (s, 3H, Me); δ_C($CDCl_3$) 157.6 (s), 155.5 (s), 152.9 (s), 145.6 (dd, 8-C), 131.4 (dt, 6-C), 118.9 (ddd, 7-C), 115.5 (dd, 9-C), 81.8 (s, 3-C), 9.74 (q, Me). The NMR assignments are based on a 2D HSQC spectrum, a DEPT and a coupled ^{13}C NMR spectrum. *m*/*z* 177 (M^+, 25%), 149 (45), 83 (100). Found C, 60.85; H, 4.27. $C_9H_7NO_3$ requires C, 61.02, H, 3.98%.

3-Phenyl-2-oxo-5λ^5-pyrido[2,1-*b*][1,3]oxazin-3-ylium-4-olate 5b

The compound was obtained as yellow crystals in 82% yield, mp 233–235 °C (lit.[8b] mp 234–236 °C, yield 73–85%); δ_H($CDCl_3$) 9.26 (d, 6-H), 8.22 (t, 8-H), 7.70 (d, 2H, arom. *ortho*), 7.51 (t, 7-H), 7.45 (d, 9-H), 7.33 (t, 2H, arom. *meta*), 7.24 (t, 1H, arom. *para*); δ_C($CDCl_3$) 156.5 (s), 155.8 (s), 152.2 (s), 146.1 (d, 8-C), 132.4 (s, phenyl 1′-C), 132.0 (br d, 6-C), 130.2 (s, phenyl *ortho*-C), 127.9 (s, phenyl *meta*-C), 126.7 (phenyl *para*-C), 118.9 (d, 7-C), 115.5 (d, 9-C), 87.2 (s, 3-C). The NMR assignments in Chart 2 are based on a 2D HSQC correlation and the GIAO-B3LYP/6-31G* calculations.

Crystals for X-ray diffraction were obtained by slow evaporation of a $CDCl_3$ solution.

2-Methoxy-4*H*-pyrido[1,2-*a*]pyrimidin-4-one 11a

Compound **11a** was prepared as previously described,[44] where its NMR assignments were also reported.

2-Methoxy-3-methyl-4*H*-pyrido[1,2-*a*]pyrimidin-4-one 11b

Compound **11b** was prepared in the same manner as **11a**[44] from 2-chloro-3-methylpyrido[1,2-*a*]pyrimidin-4-one (393 mg) and sodium (46 mg) in methanol (10 ml) under reflux for 30 min. After removal of excess methanol *in vacuo*, the crude product was taken up in methylene chloride, dried over calcium chloride, and recrystallised from methylene chloride–cyclohexane. Yield 328 mg (86%) of colourless needles. δ_H($CDCl_3$) 9.12 (dd, 1H), 7.67 (ddd, 1 H), 7.50 (dd, 1 H), 7.08 (ddd, 1 H); δ_C($CDCl_3$) 165.4, 159.0, 148.1, 135.5, 127.6, 124.7, 114.2, 94.9, 54.0, 8.7. The assignments of the NMR data given in Chart 3 are based on the B3LYP calculations. *m*/*z* 190 (100%), 162 (35), 161 (63), 78 (65). Found C, 62.99; H, 5.31; N, 14.53. $C_{10}H_{10}N_2O_2$ requires C, 63.14; H, 5.30; N, 14.73%.

2-(2-Pyridylamino)-4*H*-pyrido[1,2-*a*]pyrimidin-4-one 11c

This compound was prepared according to a literature procedure.[45] Mp 208–210 °C (lit.[45] 209–209.5 °C); GC-MS: *m*/*z* 238; ν_{max}(Ar, 28 K)/cm^{-1} 3429, 1719, 1646, 1592, 1587, 1578, 1540, 1517 1497, 1481, 1462, 1444, 1417, 1376, 1321, 1232, 1187, 1151, 774; δ_H(400.1 MHz, DMSO-d_6) 9.96 (s, 1H, NH), 8.84 (dd, $^3J_{6,7}$ 7.0, $^5J_{6,9}$ 0.8, 1H, 6-H), 8.30 (ddd, $^3J_{6',5'}$ 5.0, $^4J_{6',4'}$ 1.9, $^5J_{6',3'}$ 0.8, 1H, 6′-H), 7.85 (ddd, $^3J_{4',3'}$ 9.0, $^3J_{4',5'}$ 6.8, $^4J_{4',6'}$ 1.8, 1H, 4′-H), 7.70 (ddd, $^3J_{8,9}$ 8.4, $^3J_{8,7}$ 7.0, $^4J_{8,6}$ 1.8, 1H, 8-H), 7.56 (d, $^3J_{9,8}$ 8.4, 1H, 9-H), 7.44 (ddd, $^3J_{3',4'}$ 9.0, $^4J_{3',5'}$ 1.0, $^5J_{3',6'}$ 0.5, 1H, 3′-H), 7.15 (ddd, $^3J_{7,8}$ 6.9, $^3J_{7,6}$ 6.9, $^4J_{7,9}$ 1.3, 1H, 7-H), 6.98 (s, 1H, 3-H), 6.96 (ddd, $^3J_{5',4'}$ 7.2, $^3J_{5',6'}$ 5.0, $^4J_{5',3'}$ 1.0, 1H, 5′-H); δ_C(100.6 MHz, DMSO-d_6) 157.5, 157.5, 153.7, (C-2, C-4, C-2′), 150.3 (9a-C), 147.3 (6′-C), 137.7, 137.6 (8-C, 4′-C), 127.1 (6-C), 123.9 (3′-C), 117.2 (5′-C), 114.0 (7-C), 113.2 (9-C), 85.5 (3-C). The NMR assignments are supported by a 2D HSQC ^{1}H–^{13}C correlation for the corresponding 2-[*N*-methyl-*N*-(2-pyridyl)-amino] derivative.[46]

Acknowledgements

We thank the Karl Franzens Universität Graz for a Gandolph-Dölter Stipendium as well as the provision of a Förderungsstipendium der Naturwissenschaftlichen Fakultät for B. W., enabling her stay at the University of Queensland. We also thank Dr Colin H. L. Kennard for initial help with X-ray determinations, Mr Justin Finnerty for help with the plotting of IR spectra, and Dr Ralf Neumann for recording many NMR spectra.

References

1 A. E. Tschitschibabin, *Ber. Dtsch. Chem. Ges.*, 1924, **57**, 1168.
2 W. Friedrichsen, T. Kappe and A. Böttcher, *Heterocycles*, 1982, **19**, 1083; T. Kappe, *Lect. Heterocycl. Chem.*, 1984, **7**, 107.
3 (*a*) A. R. Katritzky and A. J. Waring, *J. Chem. Soc.*, 1962, 1544; (*b*) A. R. Katritzky, F. D. Popp and A. J. Waring, *J. Chem. Soc. B*, 1966, 565.
4 R. Urban, M. Grosjean and W. Arnold, *Helv. Chim. Acta*, 1970, **53**, 905.
5 N. Thorup and O. Simonsen, *Acta Crystallogr., Sect. C*, 1985, **41**, 472; O. Simonsen, *Acta Crystallogr., Sect. C*, 1986, **42**, 573.
6 A. Fiksdahl, C. Plüg and C. Wentrup, *J. Chem. Soc., Perkin Trans. 2*, 2000, 1841.
7 (*a*) T. Kappe and W. Lube, *Monatsh. Chem.*, 1971, **102**, 781; T. Kappe and W. Lube, *Chem. Ber.*, 1979, **112**, 3424; (*b*) T. Kappe, Y. Ravai and W. Stadlbauer, *Monatsh. Chem.*, 1983, **114**, 227; (*c*) W. Friedrichsen, T. Kappe and A. Böttcher, *Heterocycles*, 1982, **19**, 1083.
8 (*a*) T. Kappe, W. Golser, M. Hariri and W. Stadlbauer, *Chem. Ber.*, 1979, **112**, 1585; (*b*) W. Friedrichsen, E. Kujath and G. Liebezeit, *Z. Naturforsch., Teil B*, 1982, **37**, 222.
9 K. T. Potts and M. Sorm, *J. Org. Chem.*, 1971, **36**, 8.
10 H. Gotthardt and C. Flosbach, *Chem. Ber.*, 1988, **121**, 951.
11 Experimental ^{13}C NMR data for carbanions are taken from, H.-O. Kalinowski, S. Berger and S. Braun, *^{13}C-NMR-Spektroskopie*, Thieme, Stuttgart, 1984.
12 Experimental ^{13}C NMR data for pyridinium ylides are taken from, K. Matsumoto, M. Ciobanu, K. Aoyama and T. Uchida, *Heterocycl. Commun.*, 1997, **3**, 499; K. Matsumoto, H. Katsura,

T. Uchida, K. Aoyama and T. Machiguchi, *Heterocycles*, 1997, **45**, 2443.
13 X. Ye, J. Andraos, H. Bibas, M. W. Wong and C. Wentrup, *J. Chem. Soc., Perkin Trans. 1*, 2000, 401.
14 A. J. Kirby, I. V. Komarov, P. D. Wothers and N. Feeder, *Angew. Chem., Int. Ed.*, 1998, **37**, 785.
15 I. Couturier-Tamburelli, J.-P. Aycard, M. W. Wong and C. Wentrup, *J. Phys. Chem. A*, 2000, **104**, 3466.
16 C. Kratky and T. Kappe, *J. Heterocycl. Chem.*, 1981, **18**, 881.
17 T. Debaerdemaker and W. Friedrichsen, *Z. Naturforsch.*, *Teil B*, 1982, **37**, 217.
18 T. Kappe, W. Lube, K. Thonhofer, C. Kratky and U. G. Wagner, *Heterocycles*,1995, **40**, 681.
19 H. Bibas, C. H. L. Kennard and C. Wentrup, unpublished data.
20 R. Bossio, S. Marcaccini, R. Pepino and P. Paoli, *J. Heterocycl. Chem.*, 1993, **30**, 33.
21 C. Donati, W. K. Janowski, R. H. Prager, M. R. Taylor and L. M. Vilkins, *Aust. J. Chem.*, 1989, **42**, 2161.
22 H. Song, H.-S. Shin, K.-I. Park and S. I. Cho, *Acta Crystallogr., Sect. C*, 1998, **54**, 1915; M. Balogh, I. Hermecz, G. Naray-Szabo, K. Simon and Z. Meszaros, *J. Chem. Soc., Perkin Trans. 1*, 1986, 753; M. P. Gupta and K. Banerjee, *Acta Crystallogr., Sect. B.*, 1982, 2947; H. L. Ammon and G. L. Wheeler, *Acta Crystallogr., Sect. B*, 1974, **30**, 1146.
23 G. G. Qiao, J. Andraos and C. Wentrup, *J. Am. Chem. Soc.*, 1996, **118**, 5634; P. Visser, R. Zuhse, M. W. Wong and C. Wentrup, *J. Am. Chem. Soc.*, 1996, **118**, 12598.
24 W. H. De Camp and J. M. Stewart, *J. Heterocycl. Chem.*, 1970, **7**, 895; O. Gerulat, G. Himbert and U. Bergsträsser, *Synlett*, 1995, 835.
25 W. E. Thiessen and H. Hope, *J. Am. Chem. Soc.*, 1967, **89**, 5977; H. Hope and W. E. Thiessen, *Acta Crystallogr., Sect. B*, 1969, **25**, 1237; T. J. King, P. N. Preston, J. S. Suffolk and K. Turnbull, *J. Chem. Soc., Perkin Trans. 2*, 1979, 1751; S. Nespurek, J. Hasek, M. Sorm and K. Huml, *J. Mol. Struct.*, 1982, **82**, 95; J. Hasek, P. T. Beurskens, J. Obrda, S. Nespurek, H. Schenk, K. Goubitz, K. Huml and J. D. Schagen, *Coll. Czech. Chem. Commun.*, 1986, **50**, 1764; C.-H. Ueng, P. L. Lee, Y. Wang and M.-Y. Yeh, *Acta Crystallogr., Sect. C*, 1985, **41**, 1776; C.-H. Ueng, Y. Wang and M. Y. Yeh, *Acta Crystallogr., Sect. C*, 1987, **43**, 1122.
26 G. V. Boyd, C. G. Davies, J. D. Donaldson, J. Silver and P. H. Wright, *J. Chem. Soc., Perkin Trans. 2*, 1975, 1280; P. L. Toupet, F. Texier and R. Carrié, *Acta Crystallogr., Sect. C*, 1991, **47**, 328.
27 Data for 3-propionyl- and 3-acetyl[1,3]oxazolo[2,1-*b*]pyridin-4-ylium-2-olate **24** and 2-(*tert*-butyl)-3-methyl-4-(trifluoroacetyl)-munchnone **25**: C. Plüg and C. Wentrup, unpublished results.
28 S. Nespurek, S. Böhm and J. Kuthan, *J. Mol. Struct.* (*THEOCHEM*), 1986, **136**, 261; K. Undheim, M. A. F. El-Gendy and T. Hurum, *Org. Mass Spectrom.*, 1974, **9**, 1242; E. Funke and R. Huisgen, *Chem. Ber.*, 1971, **104**, 3222; J. Lukac and H. Heimgartner, *Helv. Chim. Acta*, 1979, **62**, 1236; W. Friedrichsen and W.-D. Schröer, *Liebigs Ann. Chem.*, 1980, 1836.
29 N. Harrit, A. Holm, I. R. Dunkin, M. Poliakoff and J. J. Turner, *J. Chem. Soc., Perkin Trans. 2*, 1987, 1227.
30 Ring–chain isomerism between 1-isocyanatocarbonylpyrazole and the pyrazolo[1,2-*a*][1,2,4]triazolyliumolate has been reported: A. Böttcher, T. Debaerdemaeker, J. G. Radziszewski and W. Friedrichsen, *Chem. Ber.*, 1988, **121**, 895. For other ring–chain isomerizations involving isothiocyanates, see R. M. Moriarty, R. Mukherjee, O. L. Chapman and D. R. Eckroth, *Tetrahedron Lett.*, 1971, 397; S. Chaloupka, H. Heimgartner, H. Schmid, H. Link, P. Schönholzer and K. Bernauer, *Helv. Chim. Acta*, 1976, **59**, 2566.
31 M. J. Frisch, G. W. Trucks, H. B. Schlegel, G. E. Scuseria, M. A. Robb, J. R. Cheeseman, V. G. Zakrzewski, J. A. Montgomery, Jr., R. E. Stratmann, J. C. Burant, S. Dapprich, J. M. Millam, A. D. Daniels, K. N. Kudin, M. C. Strain, O. Farkas, J. Tomasi, V. Barone, M. Cossi, R. Cammi, B. Mennucci, C. Pomelli, C. Adamo, S. Clifford, J. Ochterski, G. A. Petersson, P. Y. Ayala, Q. Cui, K. Morokuma, D. K. Malick, A. D. Rabuck, K. Raghavachari, J. B. Foresman, J. Cioslowski, J. V. Ortiz, A. G. Baboul, B. B. Stefanov, G. Liu, A. Liashenko, P. Piskorz, I. Komaromi, R. Gomperts, R. L. Martin, D. J. Fox, T. Keith, M. A. Al-Laham, C. Y. Peng, A. Nanayakkara, C. Gonzalez, M. Challacombe, P. M. W. Gill, B. Johnson, W. Chen, M. W. Wong, J. L. Andres, C. Gonzalez, M. Head-Gordon, E. S. Replogle and J. A. Pople, *Gaussian 98*, Gaussian, Inc., Pittsburgh PA, 1998.
32 (*a*) A. D. Becke, *J. Chem. Phys.*, 1993, **98**, 5648; (*b*) C. Lee, W. Yang and R. G. Parr, *Phys. Rev. B: Condens. Matter Mater.*, 1988, **37**, 785.
33 (*a*) M. W. Wong, M. J. Frisch and K. B. Wiberg, *J. Am. Chem. Soc.*, 1991, **113**, 4776; (*b*) M. W. Wong, K. B. Wiberg and M. J. Frisch, *J. Chem. Phys.*, 1991, **95**, 8991.
34 K. B. Wiberg, T. A. Keith, M. J. Frisch and M. Murcko, *J. Phys. Chem.*, 1995, **99**, 7702.
35 J. R. Cheeseman, G. W. Trucks, T. Keith and M. J. Frisch, *J. Phys. Chem.*, 1996, **104**, 5497.
36 M. W. Wong, *Chem. Phys. Lett.*, 1996, **256**, 391.
37 A. E. Reed, L. A. Curtiss and F. Weinhold, *Chem. Rev.*, 1988, **88**, 899.
38 H. L. Ammon and G. L. Wheeler, *Acta Crystallogr., Sect. B*, 1974, **30**, 1146; S. Salishi, J. L. Brianso, X. Solans and M. Font-Altaba, *Acta Crystallogr., Sect. C*, 1985, **41**, 474; M. P. Gupta and K. Banerjee, *Acta Crystallogr., Sect. B*, 1982, **38**, 2947.
39 *The XTAL3.2 User's Manual*, eds. S. R. Hall, H. D. Flack and J. M. Stewart, Universities of Western Australia, Geneva and Maryland, 1992.
40 G. M. Sheldrick, *Acta Crystallogr., Sect. A*, 1990, **46**, 467.
41 G. M. Sheldrick, *SHELXL-97: Program for Crystal Structure Determination*, University of Göttingen, 1997.
42 A. L. Spek, *Acta Crystallogr., Sect. A*, 1990, **46**, C34.
43 P. Dvortsak, G. Resofszki, L. Zalantai and A. I. Kiss, *Tetrahedron*, 1976, **32**, 2117.
44 C. Plüg, W. Frank and C. Wentrup, *J. Chem. Soc., Perkin Trans 2*, 1999, 1087.
45 G. Roma, M. Di Braccio, G. Leoncini and B. Aprile, *Farmaco*, 1993, **48**, 1225.
46 H. G. Andersen and C. Wentrup, unpublished results.